

## Supporting Information

# Small, Narrowly Distributed Iridium Nanoparticles Supported on Indium Tin Oxide for Efficient Anodic Water Oxidation

Dmitry Lebedev and Christophe Copéret\*

ETH Zurich, Department of Chemistry and Applied Biosciences, Vladimir-Prelog-Weg 1-5, CH-8093 Zurich, Switzerland

\*E-mail: [ccoperet@ethz.ch](mailto:ccoperet@ethz.ch)

## Table of Contents

<b>MATERIALS AND METHODS.....</b>	<b>3</b>
<b>EXPERIMENTAL PROCEDURES.....</b>	<b>4</b>
<b>CHARACTERIZATION DATA .....</b>	<b>4</b>
<b>REFERENCES .....</b>	<b>8</b>

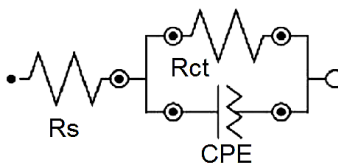
<b>Figure S1.</b> HAADF-STEM images of pristine Ir <sub>NP</sub> -ITO.....	<b>4</b>
<b>Figure S2.</b> High resolution and Fourier-transformed HAADF-STEM images of pristine Ir <sub>NP</sub> -ITO .....	<b>5</b>
<b>Figure S3.</b> CV of Ir <sub>NP</sub> -ITO recorded at 10 mV s <sup>-1</sup> , 0.1 M HClO <sub>4</sub> . .....	<b>5</b>
<b>Figure S4.</b> Tafel plot measurements of three different Ir <sub>NP</sub> -ITO electrodes.....	<b>5</b>
<b>Figure S5.</b> CV of Ir <sub>NP</sub> -ITO recorded at 10 mV s <sup>-1</sup> from 0.5 to 1.35 V vs RHE, 0.1 M HClO <sub>4</sub> . .....	<b>6</b>
<b>Figure S6.</b> HAADF-STEM images and particle size distribution of Ir <sub>NP</sub> -ITO after electrochemical surface oxidation and 20 CV cycles from 0.5 to 1.35 V vs RHE (10 mV s <sup>-1</sup> , 0.1 M HClO <sub>4</sub> ).....	<b>6</b>
<b>Figure S7.</b> HAADF-STEM images of Ir <sub>NP</sub> -ITO after 2 h @ 10 mA cm <sup>-2</sup> . .....	<b>6</b>
<b>Figure S8.</b> High resolution and Fourier-transformed HAADF-STEM image of Ir <sub>NP</sub> -ITO after 2 h @ 10 mA cm <sup>-2</sup> with the overlaid interplanar distances and projection of Ir metal structure. ....	<b>7</b>
<b>Figure S9.</b> Survey XPS spectra of pristine Ir <sub>NP</sub> -ITO and Ir <sub>NP</sub> -ITO after 2 h @ 10 mA cm <sup>-2</sup> .....	<b>7</b>

## Materials and methods

Iridium trichloride hydrate (99.9%–Ir) was obtained from Strem, ITO powder was obtained from Evonik (VP ITO TC8), polyvinylpyrrolidone (PVP, 40 kDa) and hydroxypropyl cellulose (HPC, average  $M_w$  ca. 80000, 20 mesh particle size) were obtained from Sigma Aldrich. Fluorine-doped tin oxide (FTO) coated glass substrates were obtained from Solaronix.

Powder X-ray diffraction experiments were performed on PANalytical X'Pert PRO MPD diffractometer using Cu  $K_\alpha$  radiation. High-angle Annular Dark Field Scanning Transmission Electron Microscopy (HAADF–STEM) imaging was performed using an aberration-corrected JEOL JEM-ARM 200CF transmission electron microscope operated at 200 kV. Elemental analysis was performed by the Mikroanalytisches Labor Pascher; Remagen, Germany. X-ray photoelectron spectroscopy (XPS) measurements were performed using a VG ESCALAB 220iXL spectrometer (Thermo Fischer Scientific) equipped with an Al  $K_\alpha$  monochromatic source (15 kV/ 150 W, 500  $\mu$ m beam diameter) and a magnetic lens system. The binding energies of the acquired spectra were referenced to the C 1s line at 284.8 eV. Background subtraction was performed according to Shirley.<sup>1</sup> Fitting of the Ir 4f XPS peaks was performed using CasaXPS software with the asymmetric Lorentzian lineshape LF(1,2,10,20).

Electrochemical measurements were performed in a standard single-compartment 3-electrode cell using PGSTAT128N Autolab potentiostat. The porous ITO electrodes were electrically contacted using the uncoated FTO layer and masked to a geometrical surface area of 1.5 cm<sup>2</sup>. A piece of a platinum mesh served as the counter electrode and saturated Ag/AgCl electrode served as the reference electrode. 0.1 M HClO<sub>4</sub> electrolyte was saturated with Ar prior to the measurements. Cyclic voltammograms (CVs) were recorded in the potential range of 0.46 – 1.56 V vs RHE at 10, 25 and 50 mV s<sup>-1</sup> (starting with the 20 CV cycles at 25 mV s<sup>-1</sup>, with the first cycle in the anodic direction, Figure 2a). Electrochemical impedance spectroscopy measurements were recorded at 1.46 V vs RHE with an amplitude of 10 mV in the range of 10 kHz to 10 mHz. Electrochemical impedance spectroscopy data (Nyquist plot) were fitted using the equivalent circuit consisting of resistor (solution ohmic drop) in series with parallel resistor (charge transfer) and constant phase element:



Polarization curves were obtained from the steady-state chronoamperometric measurements: the potential was gradually stepped from 1.41 to 1.61 V vs RHE (with 25 mV steps) while holding for 1 min at each potential. Average of the last 10 s of the current for each potential step and solution ohmic drop corrected potentials were used for Tafel plot construction (Fig. S4). For the stability measurements the potentiostat was switched to the galvanostatic mode (chronopotentiometry) and 10 mA cm<sup>-2</sup> current was maintained for two hours. Both vigorous stirring and argon bubbling of electrolyte were used for chronoamperometric and chronopotentiometric measurements. All reported measurements were repeated several times to ensure the reproducibility of the results. All the

potential values are reported vs Reversible Hydrogen Electrode (RHE) scale. The current expressed as  $[\text{mA cm}^{-2}]$  refers to the geometrical surface area of the electrode and  $[\text{A g}_{\text{Ir}}^{-1}]$  refers to the total mass of Ir on the electrode, determined using elemental analysis.

## Experimental procedures

The porous ITO electrodes were prepared by depositing a paste containing 5 wt. % of hydroxypropyl cellulose and 10 wt. % of ITO powder in ethanol on cleaned FTO-coated glass using the Doctor Blade method.<sup>2-3</sup> The electrodes were subsequently calcined at 500 °C for 1 hour (with a ramp of 60 °C h<sup>-1</sup>). Colloidal Ir nanoparticles were prepared via a solvothermal method by heating iridium trichloride hydrate in ethylene glycol at 200 °C for 24 hours in the presence of polyvinylpyrrolidone.<sup>4</sup> The particles were subsequently purified via cyclohexane precipitation followed by an ethanol redissolution.

For the deposition of Ir nanoparticles on porous ITO electrodes (to produce Ir<sub>NP</sub>-ITO), 1.67 mL of the ethanolic colloidal solution of Ir nanoparticles (approx. 50 mM Ir) were adjusted to 10 mL with 0.1 M HClO<sub>4</sub>. Twelve freshly calcined ITO electrodes were immersed in the obtained solution (in a Petri dish) for 16 hours. After particle immobilization electrodes were washed 3 times with 0.1 M HClO<sub>4</sub> and once with DI water and finally dried in air.

Iridium loading was calculated using the following equations:

$$\text{Ir loading, } [\text{mol cm}^{-2}]: N_{\text{Ir}} = \frac{\omega_{\text{Ir}} m_{\text{cat}}}{(100 - \omega_{\text{Ir}}) M_{\text{Ir}}};$$

$$\text{Ir loading, } [\text{g cm}^{-2}]: m_{\text{Ir}} = \frac{\omega_{\text{Ir}} m_{\text{cat}}}{(100 - \omega_{\text{Ir}})};$$

where  $\omega_{\text{Ir}}$  is weight loading of Ir, found to be 4.1 % by elemental analysis;

$M_{\text{Ir}}$  is Ir molecular weight;

$m_{\text{cat}}$  is the catalyst loading on the electrode, found to be 2.4 mg cm<sup>-2</sup>.

## Characterization data

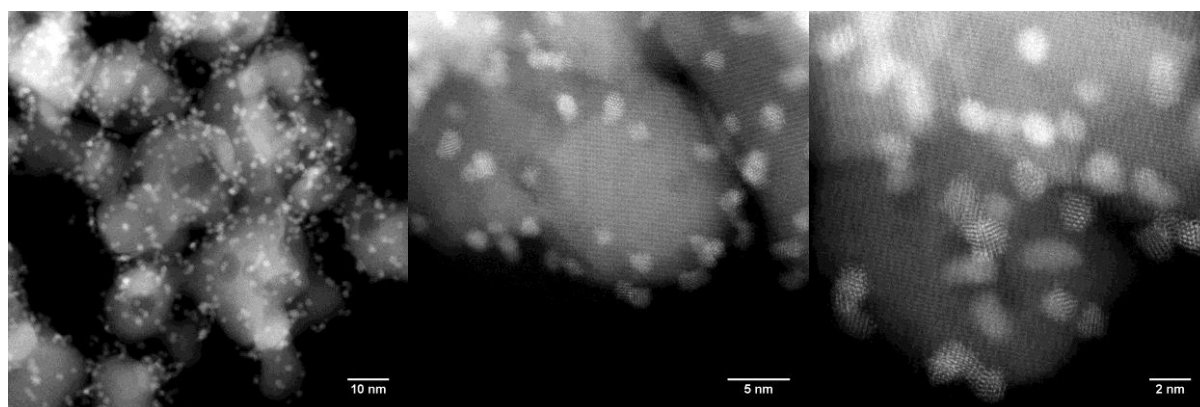


**Figure S1.** HAADF-STEM images of pristine Ir<sub>NP</sub>-ITO.

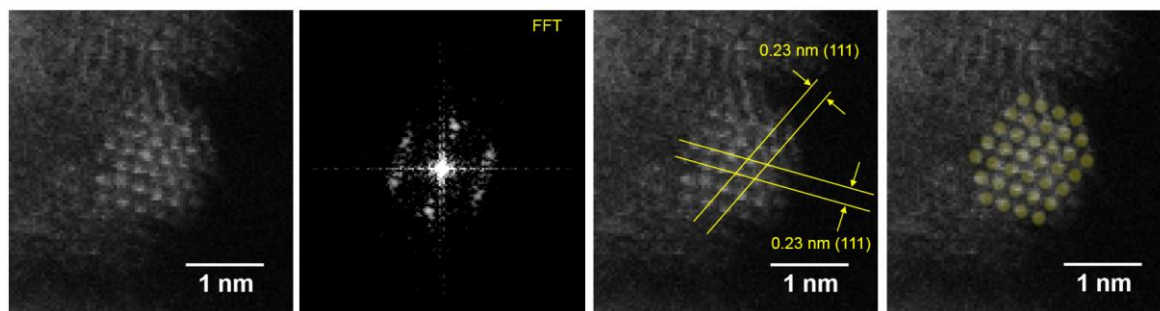


**Figure S2.** High resolution and Fourier-transformed HAADF-STEM images of pristine Ir<sub>NP</sub>-ITO with the overlaid interplanar distances and projection of Ir metal structure.

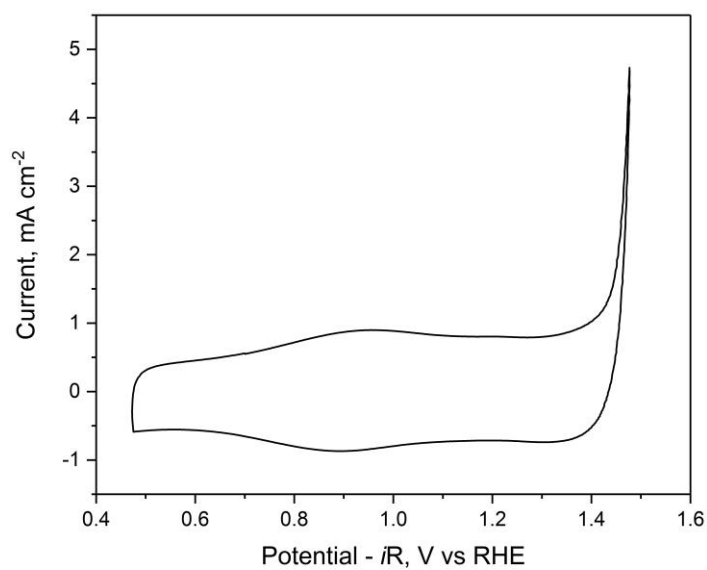


**Figure S3.** CV of Ir<sub>NP</sub>-ITO recorded at 10 mV s<sup>-1</sup>, 0.1 M HClO<sub>4</sub>.

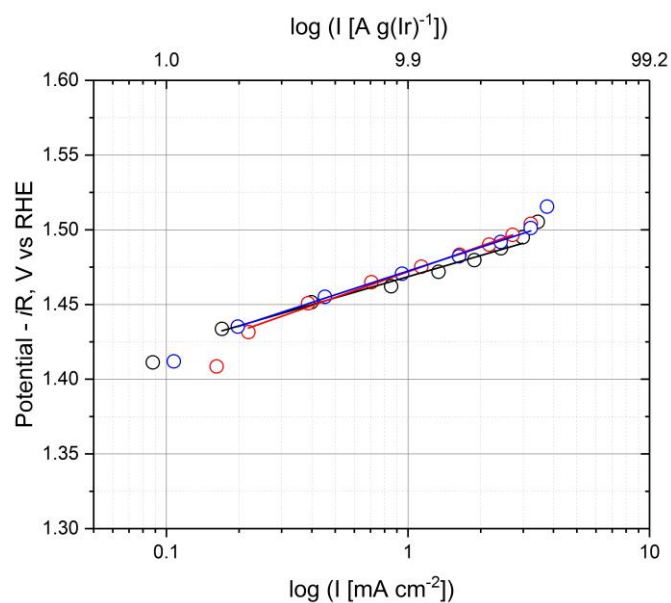


**Figure S4.** Tafel plot measurements of three different Ir<sub>NP</sub>-ITO electrodes. The average Tafel slope is  $52 \pm 5$  mV dec<sup>-1</sup>.

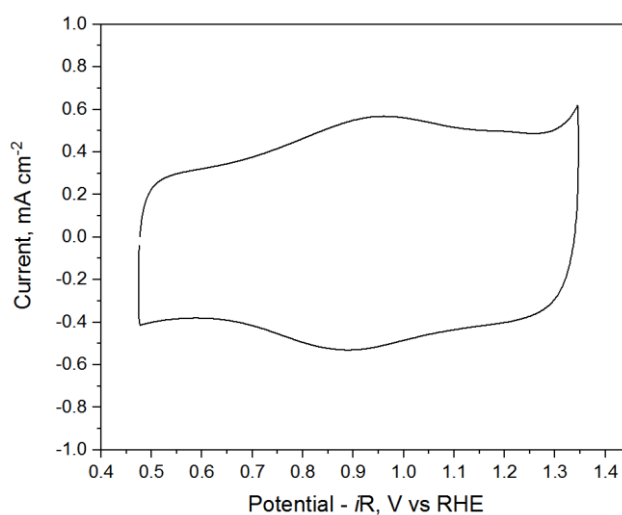


**Figure S5.** CV of Ir<sub>NP</sub>-ITO recorded at 10 mV s<sup>-1</sup> from 0.5 to 1.35 V vs RHE, 0.1 M HClO<sub>4</sub>. This sample was subsequently analysed using STEM-HAADF (Figure S6).

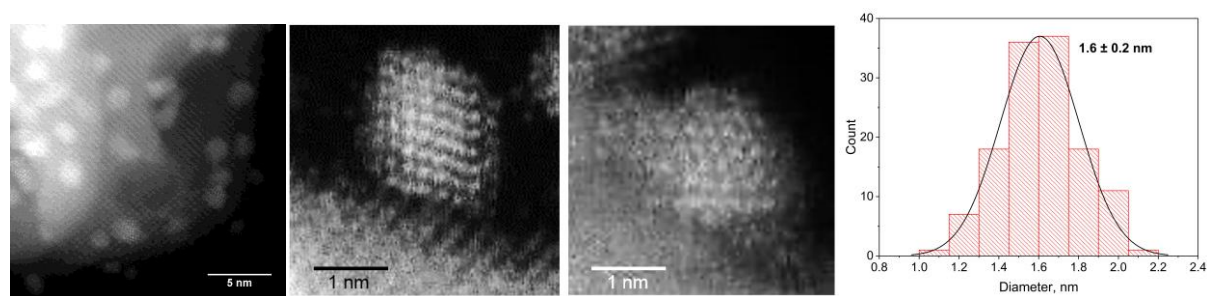


**Figure S6.** HAADF-STEM images and particle size distribution of Ir<sub>NP</sub>-ITO after electrochemical surface oxidation and 20 CV cycles from 0.5 to 1.35 V vs RHE (10 mV s<sup>-1</sup>, 0.1 M HClO<sub>4</sub>, Figure S5).

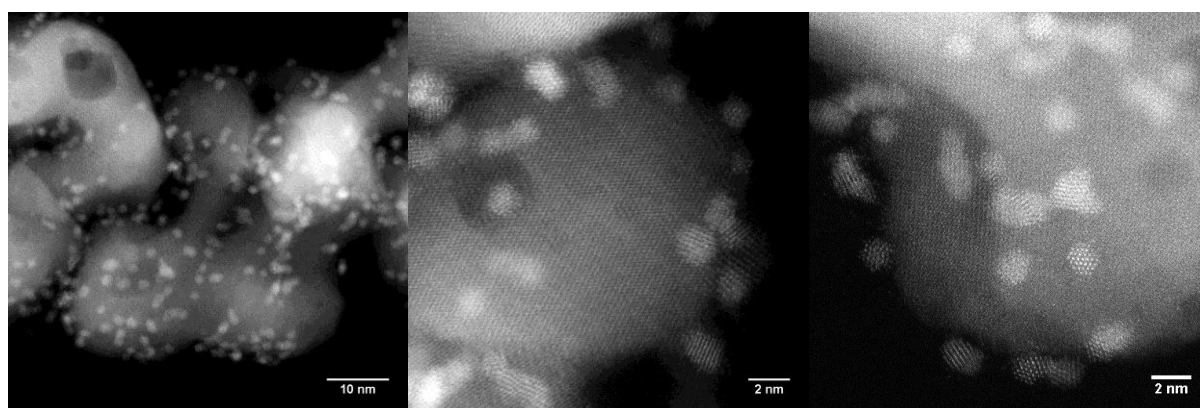


**Figure S7.** HAADF-STEM images of Ir<sub>NP</sub>-ITO after 2 h @ 10 mA cm<sup>-2</sup>.

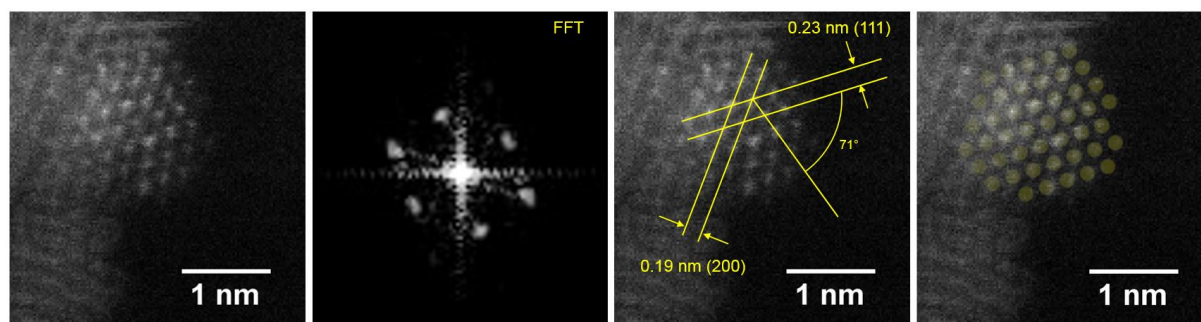


**Figure S8.** High resolution and Fourier-transformed HAADF-STEM image of Ir<sub>NP</sub>-ITO after 2 h @ 10 mA cm<sup>-2</sup> with the overlaid interplanar distances and projection of Ir metal structure.

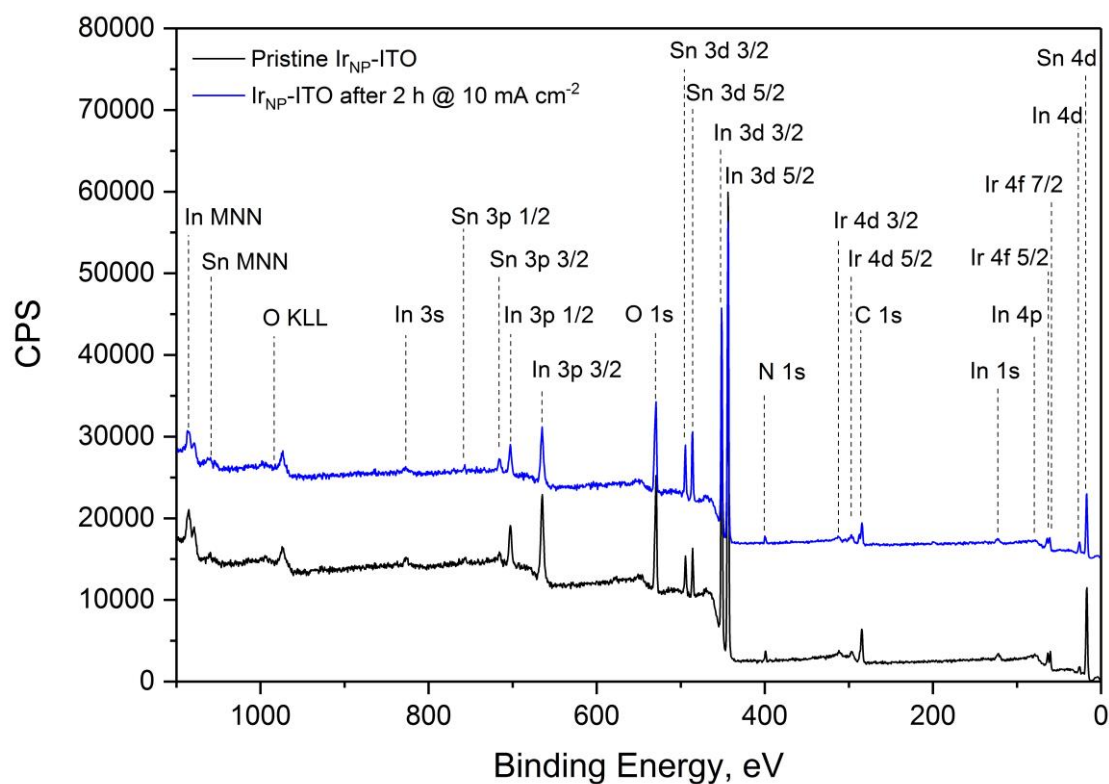


**Figure S9.** Survey XPS spectra of pristine Ir<sub>NP</sub>-ITO (black) and Ir<sub>NP</sub>-ITO after 2 h @ 10 mA cm<sup>-2</sup> (blue).

## References

1. Shirley, D. A., High-Resolution X-Ray Photoemission Spectrum of the Valence Bands of Gold. *Phys. Rev. B* **1972**, *5*, 4709-4714.
2. Farnum, B. H.; Morseth, Z. A.; Brennaman, M. K.; Papanikolas, J. M.; Meyer, T. J., Driving force dependent, photoinduced electron transfer at degenerately doped, optically transparent semiconductor nanoparticle interfaces. *J. Am. Chem. Soc.* **2014**, *136*, 15869-15872.
3. Lebedev, D.; Pineda-Galvan, Y.; Tokimaru, Y.; Fedorov, A.; Kaeffer, N.; Coperet, C.; Pushkar, Y., The Key Ru(V)=O Intermediate of Site-Isolated Mononuclear Water Oxidation Catalyst Detected by in Situ X-ray Absorption Spectroscopy. *J. Am. Chem. Soc.* **2018**, *140*, 451-458.
4. Zhang, T.; Li, S.-C.; Zhu, W.; Ke, J.; Yu, J.-W.; Zhang, Z.-P.; Dai, L.-X.; Gu, J.; Zhang, Y.-W., Iridium ultrasmall nanoparticles, worm-like chain nanowires, and porous nanodendrites: One-pot solvothermal synthesis and catalytic CO oxidation activity. *Surf. Sci.* **2016**, *648*, 319-327.